This article has been accepted for publication in a future issue of this journal, but has not been fully edited. Content may change prior to final publication. Citation information: DOI 10.1109/JSTQE.2018.2854566, IEEE Journal of Selected Topics in Quantum Electronics

Machine learning optimization of surface-normal optical modulators for SWIR time-of-flight 3D camera

Simone Bianconi, Skyler Wheaton, Min-Su Park, Iman Hassani Nia and Hooman Mohseni

***Abstract*— Surface-normal optical modulators based on multiple quantum wells are attractive for an increasing number of applications, including photonic links such as on-chip optical interconnects. The design of such structures however, is still based on intuition and experience rather than on a quantitative assessment of the device and system performance, due to the extreme complexity of the device behavior and the large number of design parameters involved. We developed a method for the systematic optimization of the modulator design, using a combination of analytical modeling and supervised machine learning. The global optimization is driven by an evolutionary algorithm, and the robustness of the final results is evaluated using variance-based sensitivity analysis. The optimization algorithm was tested on the case of time-of-flight 3D camera (ranging) application, yielding two novel optimized designs which allow for a considerable improvement of the depth resolution of the system. Finally, we propose a figure of merit for comparing the modulation efficiency of surface-normal modulators.**

I. INTRODUCTION

Surface-normal optical modulators are attractive for a wide range of applications, including free-space communication [1] and ranging systems [2], protection of optoelectronic sensors from laser glare [3], [4] and photonic links [5]. In particular, modulators operating around telecommunication wavelength (1550 nm) are attracting increasing interest for their potential application in chip-to-chip optical interconnect, including large area modulators [6] and arrays of them [7].

Multiple quantum well (QW) structures of III-V semiconductors constitute the most effective platform for surface-normal electro-asborptive modulators, especially for operating frequencies above hundreds of KHz [8]. However, conventional rectangular quantum wells (RQW) modulators based on quantum-confined Stark effect [9] require a very high voltage for a considerable change of absorption [10]. To address this issue, two alternative designs of the QW structure have been proposed: coupled quantum wells (CQW) and stepped quantum wells (SQW) (Figure 1).

Coupled quantum wells consist of two rectangular quantum wells separated by a thin barrier, such that the wavefunctions can couple through tunneling. In these structures the resonant coupling of the energy levels in the wells allows for an abrupt change in the overlap of the wavefunctions, resulting in a considerable change of absorption for a relatively small change in applied bias [11]. Figure 1a shows the simulated band structure and first bound wavefunctions of the CQW design reported by Stievater et al. [5], which we here refer to as *Design A*. Despite being largely employed for a wide range of applications, CQW modulators suffer from an extremely limited optical bandwidth inherent to the resonant nature of the electro-absorptive behavior [8]. This limitation is particularly stringent for some applications, since a change in temperature will result in a shift of the bandgaps, hindering the performance of the device at the wavelength range of interest.

Stepped quantum wells, on the other hand, are based on layers of graded composition arranged in such fashion as stair steps, so as to form an asymmetric well profile which induces a spatial separation between the wavefunctions [12]. Compared to CQW, this design offers the advantage of a large optical bandwidth: thanks to the gradual change in wavefunctions overlap, which can be controlled by the electric field, this design allows for a high tunability of the operating wavelength. For this reason, electro-absorptive modulators based on SQW can be operated over a large range of temperatures by simply adjusting the applied bias [8]. The simulated band structure and bound wavefunctions of a previously reported SQW design [8] is shown in Figure 1b: throughout the paper this design will be referred to as *Design B*.

Although the characteristics and advantages of both types of QW designs have been widely investigated, nonetheless the design of these structures mostly relies on intuition and experience, rather than on a quantitative evaluation of the device and system performance. This is because it is often impossible to find a straightforward relation for guiding the design, due to the large number of parameters to optimize and their strong correlation. For instance, it has been shown that increasing the thickness of the electro-active region (i.e. the optical path) improves the depth of modulation (DoM) of the device, provided the absorption loss across the modulator is low in the high-transmission mode [13]. However, increasing the thickness of the device also lowers the effective field across each quantum well, for a fixed applied bias. Hence, for any given QW design there is an optimal device thickness, which in turn depends on the electro-optical properties of the QW structure.

We propose an optimization method for the application-oriented design of electro-absorptive modulators, based on the integration of machine learning and analytical modeling of the absorption spectrum. In recent years, machine learning has been applied to an increasing number of scientific fields, including opto-electronics [14]-[16]. In particular, supervised machine learning integrated with an analytical model was implemented to tackle optimization problems with a large parameter space and high computational load [17]. The main advantage of machine learning is its ability to perform a global optimization of a highly nonlinear function over a large parameter space without the need of excessive computational power. The proposed approach is highly versatile, since it can be applied to any material system of which the basic

This article has been accepted for publication in a future issue of this journal, but has not been fully edited. Content may change prior to final publication. Citation information: DOI 10.1109/JSTQE.2018.2854566, IEEE Journal of Selected Topics in Quantum Electronics

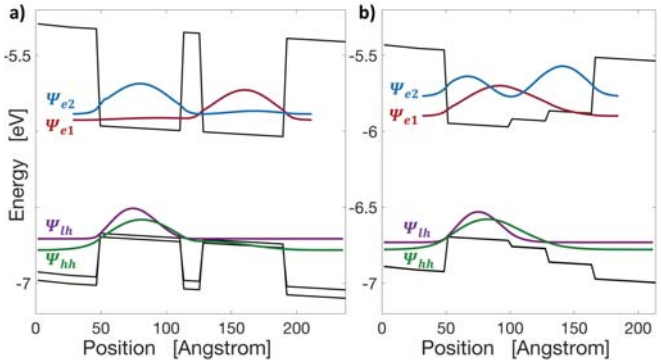

Figure 1 Simulated band structure and bound wavefunctions of CQW Design A [5] (a) and SQW Design B [8] (b) at 50 kV/cm field. The first two bound electron wavefunctions (Ψ_{e1} and Ψ_{e2}), both the heavy hole (Ψ_{hh}) and the light hole (Ψ_{lh}) wavefunctions are reported.

electronic and optical properties are known, as well as to any application of which a performance figure of merit has been defined. Moreover, the developed algorithm includes a sensitivity analysis to evaluate the robustness of the optimization with respect to small deviations caused by non-idealities inherent to the growth and fabrication methods.

To test the validity and efficacy of the proposed approach, we consider the performance of surface-normal optical modulators used in a continuous wave (CW) time-of-flight (ToF) 3D camera system operating in the short wavelength infrared (SWIR). In a recent work [18] our group has demonstrated a ToF system based on a large-area electro-absorptive modulator integrated with a commercial SWIR camera, operating at higher frequency than currently available technology [2], [19]. A schematic of the system is reported in Figure 2. Using the implemented optimization algorithm, we generated several modulator designs optimized for the application in a ToF 3D camera system and evaluated their robustness and feasibility. We then selected and investigated two of the optimized designs: a coupled-quantum well design (*Design A2*) and a stepped-quantum well design (*Design B2*). Both designs show a better performance than the respective previously published designs (*Design A* and *Design B*) [5], [8].

II. METHODS

A. Optimization parameters

The depth resolution of a CW ToF system can be estimated by [2]:

$$\Delta L = \frac{1}{2\sqrt{8}} \frac{c}{2 f_{MOD}} \frac{\sqrt{N_D + N_{BG} + N_{OBJ}}}{K N_{OBJ}} \qquad (1)$$

where c is the speed of light, f_{MOD} is the modulation frequency, N_D is the noise counts due to dark current and read noise, N_{BG} and N_{OBJ} represent the counts due to the optical signal coming from the background scene and the observed object respectively. K is the system modulation contrast, defined as the product of the depth of modulation (DoM) of the illumination source and of the modulator. Since the former is usually close to 100%, the modulation contrast of the system is mostly determined by the DoM of the modulator, which can be expressed as $DoM = \frac{|T_{V=V_1} - T_{V=V_2}|}{\max(T_{V=V_1}, T_{V=V_2})}$, where T is the transmission across the modulator. The optical signal counts are proportional to the quantum efficiency of the camera, its integration time, the energy of the photons hc/λ, and the optical power collected at the camera, P_{OPT}. As represented in Figure 2a, the light returning from the illuminated scene is collected by a lens and sent across the modulator before being collected at the camera; because of the reflection and absorption in the modulator, P_{OPT} can be expressed as a function of the optical power collected at the system aperture, P_{COLL}, as:

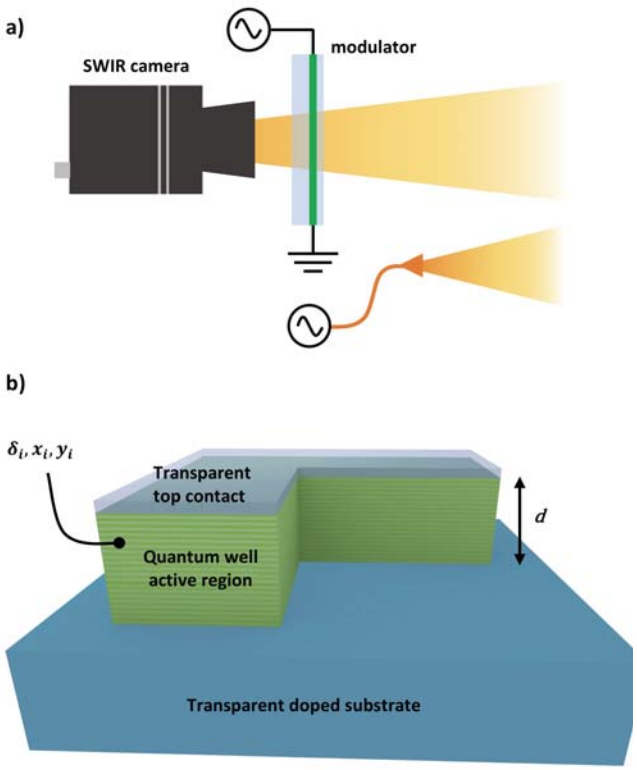

Figure 2 a) Schematic of the time-of-flight camera system including the surface-normal optical modulator; b) Schematic of the device structure and cross section reporting the device parameters used in the optimization

$$P_{OPT} = (1 - R)\, P_{COLL}\, e^{-\alpha \ell} \qquad (2)$$

where R is the reflectivity at the modulation interfaces, α is the absorption coefficient in the modulator, and ℓ is the optical pathlength across the modulator.

Figure 2b shows a schematic of the layered structure of the device: the thickness and area of the modulator (d, A) as well as the applied DC bias and voltage swing (V_{DC}, V_{AC}) are device-level optimization parameters; the thicknesses (δ_i) and compositions (x_i, y_i) of the layers in the QW structure, as well as their number, sequence and material system, are parameters of the QW design. For a single-pass, low-NA system, the optical length ℓ fundamentally reduces to the thickness of the modulator's active region, d, since the

This article has been accepted for publication in a future issue of this journal, but has not been fully edited. Content may change prior to final publication. Citation information: DOI 10.1109/JSTQE.2018.2854566, IEEE Journal of Selected Topics in Quantum Electronics

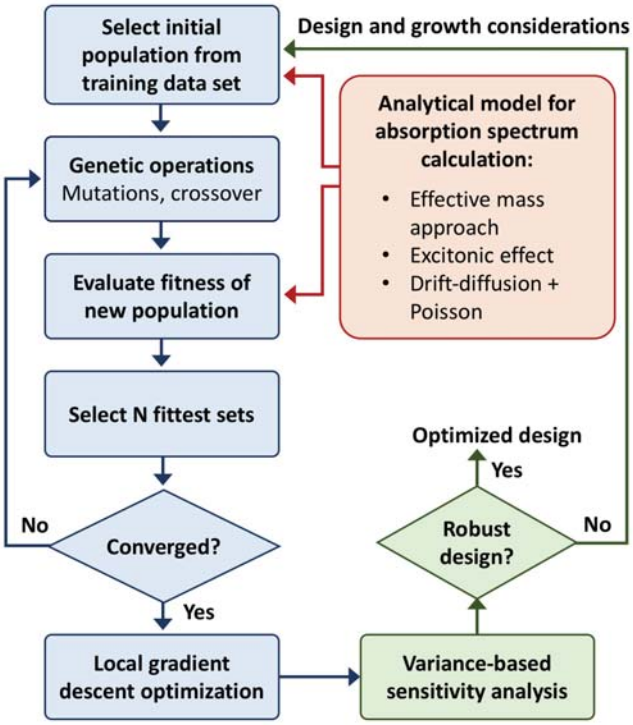

Figure 3 Schematic of the evolutionary algorithm implemented for the global optimization. The blocks in blue represent the genetic algorithm, those in green the variance-based sensitivity analysis, and the red block the analytical model.

electrodes and substrate are transparent in the wavelength range of interest. Conversely, the absorption coefficient is a complex function of many of these parameters, since it depends both on the QW design, on the field across the active region, $E = {(V_{DC} + V_{AC})}/{d}$, and other environmental variables such as the temperature T: $\alpha = \alpha\,(\delta_i, x_i, y_i, E, T)$.

Another indicator of the system performance is the power required to drive the modulator load, which is related to the capacitance (and hence the area and thickness) of the modulator. Therefore, for the purpose of the optimization, a cost function can be defined as: $\Delta = \Delta L\, f(P)$, where $f(P)$ is a non-linear function of the power consumption, defined in relation to the operating conditions of the envisaged application (operating temperature, heat sink, etc.). Such cost function is to be minimized for optimizing the modulator design for 3D ToF camera application.

B. Optimization technique

Several optimization parameters have a non-linear effect on the performance of the modulator and a strong interaction between the parameters prevents an optimization of each of them individually. Therefore the shape of the Δ cost function in the parameter space is fairly complex and presents several local minima. In such scenario, deterministic optimization techniques such as gradient descent or simplex algorithm are typically unfit for finding the global minimum, as the optimization will settle in the local minimum which is closest to the initial guess.

We developed an evolutionary global optimization technique based on a genetic algorithm (GA) trained on a dataset from an analytical model, used in conjunction with local optimization performed using gradient descent. The training data set was obtained from simulations of different QW structures, performed using an analytical model that computes the optical absorption spectrum of the QW structure using an effective mass approach, including the excitonic effect which is calculated using a variational method [10]. The field across the QW is obtained from the applied voltage and the device total thickness using drift-diffusion and Poisson's equations. The model was validated against several experimental results in previous works by our group [8], [10], [12], [13], [19], [20]. Since available experimental data is relatively scarce for such a large parameter space, the analytical model allows to expand the size of the training set to guarantee the statistical significance of the training of the GA, as proposed in [17].

Figure 3 shows a schematic of the developed optimization strategy: starting from a sampling of the training data set, the evolutionary algorithm generates an initial population of N parameter sets that define a specific modulator design (individuals) and performs genetic operations on them, such as mutation and crossover. The new population of individuals is then tested for fitness using the Δ cost function and the N fittest individuals are selected for surviving onto the next generation. This operation is repeated until a satisfactory value of the Δ cost function is reached by some of the fittest individuals, at which point a gradient descent optimization is employed to speed up the convergence to the local minima of each of the final designs.

The search of the parameter space is guided by physical principles that impose some constraint on the optimization parameters. For instance, lattice matching with the chosen substrate introduces a constraint on the composition of every layer of the structure, while the maximum applied voltage needs to be always maintained below the breakdown field of the materials, imposing a limit in the relation between the operating voltage and the device thickness. Moreover, considering that the device is designed for operation at the 1550 nm telecom wavelength, the optimization needs to account for the effect of temperature on the bandgap of the chosen materials in the desired temperature range of operation. Finally, the number of degrees of freedom of the optimization can be varied depending on design and growth considerations, which may impose limitations on the thicknesses, number and sequence of the layers as well as on the material systems. On the other hand, if some of these constraints are lifted, the evolutionary algorithm free is left free of exploring more novel design concepts.

In order to account for the deviations from design that are inherent with the material growth, the robustness of each of the final designs was assessed using Sobol variance-based sensitivity analysis [21]. A sampling population of 100 parameter sets was constructed by perturbing each of the finalized designs; the Sobol sequence was used to effectively cover the entire range of variability. The performance of each of these new sampling points was evaluated using the Δ cost function, and the estimators proposed by Saltelli et al. [22]

This article has been accepted for publication in a future issue of this journal, but has not been fully edited. Content may change prior to final publication. Citation information: DOI 10.1109/JSTQE.2018.2854566, IEEE Journal of Selected Topics in Quantum Electronics

were used to compute the main and total Sobol indices. The data from the variance-based sensitivity analysis also allowed to estimate the stability radius [23] of each of the parameters in order to evaluate the maximum tolerable deviation from design for every of the final optimized structures. The Sobol indices and the stability radius were used as indicators of the robustness of the optimized designs, in order to make considerations on the risk associated with the growth of the structures.

III. RESULTS

A. Optimized designs

Using the optimization algorithm, the two modulator designs presented in Figure 1 were optimized for the application in a ToF 3D camera system.

The first optimized structure (*Design A2*) is a CQW similar in concept to *Design A*. However, having a material system consisting of ternaries with only one element from group V is known to be beneficial to the quality of the growth, due to the competition between elements of the group V [24]. For this reason, this design was optimized fixing the material systems to only GaInAs and AlInAs, lattice-matched to InP. Furthermore, a lower limit on the thickness of the thin barrier was imposed, to avoid severe deformations of the barrier due to material interdiffusion [10]. All the other parameters were left free in the optimization, including the thicknesses of both the coupled quantum well, yielding an asymmetric CQW design.

The second optimized structure (*Design B2*) was obtained from the SQW *Design B* fixing the layout of the structure (i.e. the material system, layer number and sequence) and optimizing the remaining parameters such as thickness and composition of the QW layers. The calculated power consumption at 150 MHz and depth resolution for each of these two structures are compared with the previously published structures of the same type [18] Table I.

TABLE I
PERFORMANCE OF OPTIMIZED DESIGNS AT 300 K, 5 V SWING

Design	Power consumption at 150 MHz	Depth resolution
A	0.71 W	16.1 cm
A2	0.21 W	3.9 cm
B	0.27 W	12.4 cm
B2	0.26 W	10.5 cm

Both designs enable an improvement in the depth resolution of the system: *Design A2* shows an improvement of >75% with respect to *Design A*, and *Design B2* of >15% with respect to *Design B*.

In order to compare the modulation efficiency of the optimized QW designs in a broader perspective, we consider the depth resolution of a shot noise-limited system (i.e. $N_{OBJ} \gg N_{BG}, N_D$, corresponding to high-illumination and low-background noise). In this regime, equation (1) simplifies to:

$$\Delta L = \frac{c}{2\sqrt{8}} \frac{1}{f_{MOD}\ DoM\ N_{OBJ}} \qquad (3)$$

where the DoM of the modulator replaced K, since the DoM of the illumination source was assumed to be 100%. Furthermore, assuming a small reflection at the surface (thanks for example to anti-reflection coating), N_{OBJ} can be approximated by the transmission across the modulator, T. The power consumption for driving the modulator can be expressed as:

$$P = f_{MOD}\ C\ V_{AC}^2 \qquad (4)$$

where C represents the capacitance per unit area of the modulator, which depends on its thickness. Multiplying (3) and (4), f_{MOD} cancels out, yielding the following expression for the modulation efficiency versus power consumption:

$$Eff = \frac{DoM\ T}{C\ V_{AC}^2} \qquad (5)$$

This figure of merit expresses the amplitude of modulation [2] per unit of energy consumed per unit area, and thus has units of $J^{-1}\ mm^2$. In order to compare the performance of surface-normal modulators in transmission or reflection mode (i.e. single or double pass absorption) to those using a cavity, we have to take into account the number of modes that can be modulated per unit area by a given device. Multiplying the modulation efficiency by the number of modes per unit area, we obtain the figure of merit:

$$FoM = \frac{DoM\ T}{A_{MODE}\ C\ V_{AC}^2} \qquad (6)$$

where the unit of area cancel out, yielding the number of modes that are being modulated per Joule.

TABLE II
PERFORMANCE OF SURFACE-NORMAL QW MODULATOR DESIGNS

Design	Power consumption at 1 GHz	FoM [#modes/pJ]
A	4.7 W	234
A2	1.4 W	796
B	1.8 W	208
B2	1.7 W	233
Wang *et al.* [26]	2.3 W	178
Clare *et al.* [27]	12 W	26
Ristic *et al.* [28]	12 W	72
*Stievater *et al.* [29]	36 W	$1.2\ 10^{-3}$
*Audet *et al* [30]	5.7 W	$5.5\ 10^{-4}$

* Cavity-based surface-normal modulator

This article has been accepted for publication in a future issue of this journal, but has not been fully edited. Content may change prior to final publication. Citation information: DOI 10.1109/JSTQE.2018.2854566, IEEE Journal of Selected Topics in Quantum Electronics

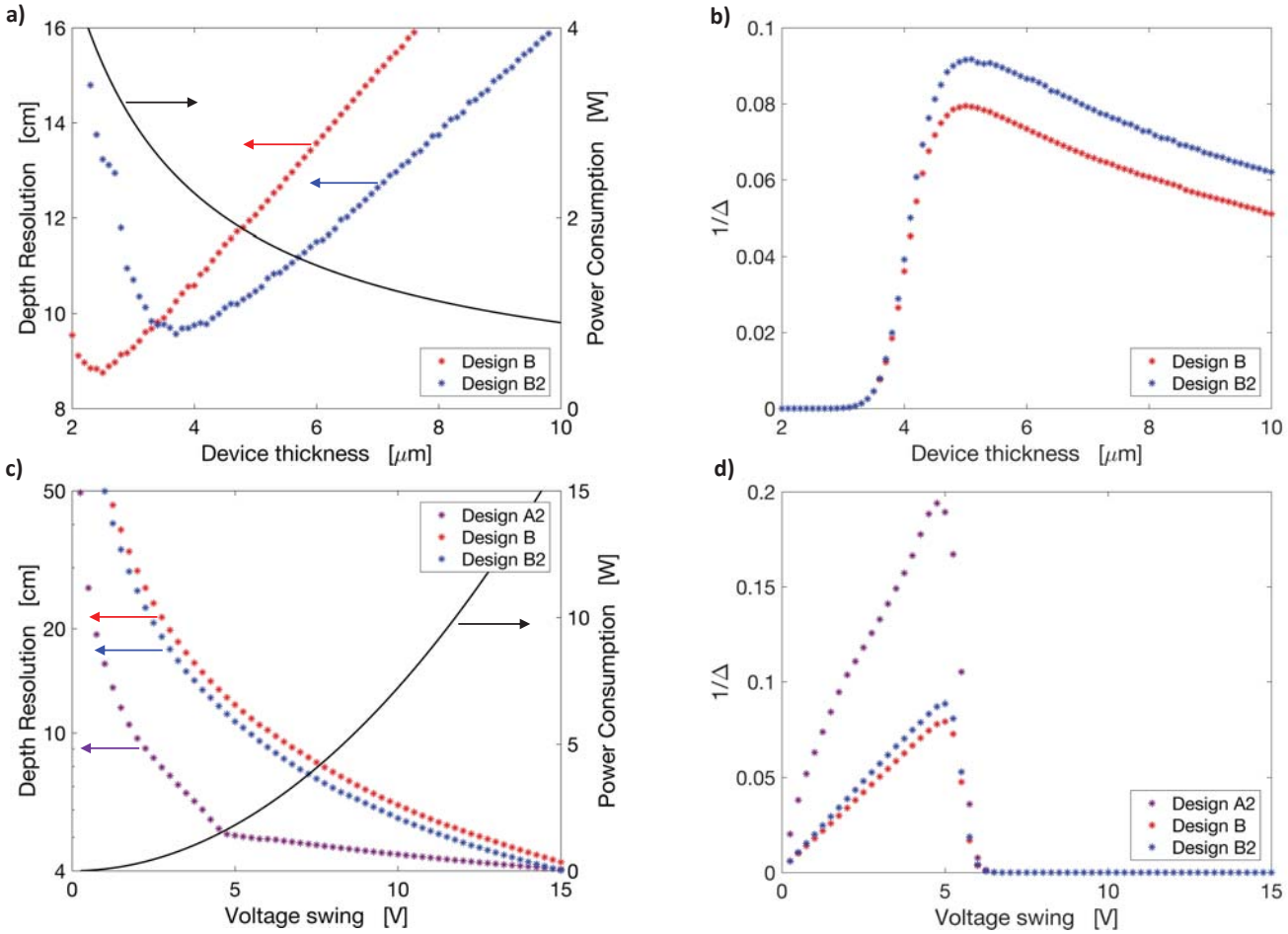

Figure 4 a) Simulation results representing the effect of the device thickness on the power consumption of the device (solid black line), and on the depth resolution of the ToF camera system for Design B and B2; b) Optimization cost function, Δ, for both designs also as a function of the device thickness. c) Simulated depth resolution of the ToF camera system and power consumption (solid black line) for driving the modulator as a function of voltage swing for three modulator designs (A2, B, B2); d) Corresponding optimization cost function, Δ, all designs also as a function of the device thickness. The cost function utilized is defined as $\Delta = \Delta L\ (1 + e^{8\,(P-2.2)})$*, and for visualization purposes it is plotted as* $1/\Delta$ *such that optimum corresponds to the max of the curves.*

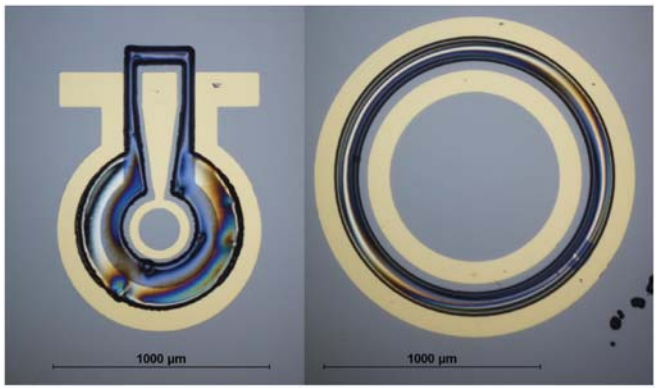

Figure 5 Microscope images of the modulator devices, fabricated for use in ToF camera application

Using the above-mentioned figure of merit, the performances of the optimized designs were compared with that of the reference designs, *A and* B as well as of several published designs, as reported in Table II. The power consumption for a modulation frequency of 1 GHz and the maximum DoM are also reported for each device.

To further characterize the modulation efficiency of the optimized designs, we investigated their performance in terms of power consumption, and compared it with that of *Design A* and *B*. Figure 4a reports the power consumption and depth resolution of *Design B* and *B2* as a function of the total device thickness, d. While the power consumption is inversely proportional to the device thickness ($C = {}^{\varepsilon A}/_{d}$), the effect of the thickness on the depth resolution is dual. On one hand, a higher total thickness of the modulator absorbing region increases the effect of a change in the absorption coefficient $\alpha = \alpha(V)$, hence increasing the DoM. On the other hand, a decrease in device thickness results in a larger field across each QW for a given applied voltage, hence increasing the Stark shift of the bound wavefunctions in the well and improving the DoM.

This article has been accepted for publication in a future issue of this journal, but has not been fully edited. Content may change prior to final publication. Citation information: DOI 10.1109/JSTQE.2018.2854566, IEEE Journal of Selected Topics in Quantum Electronics

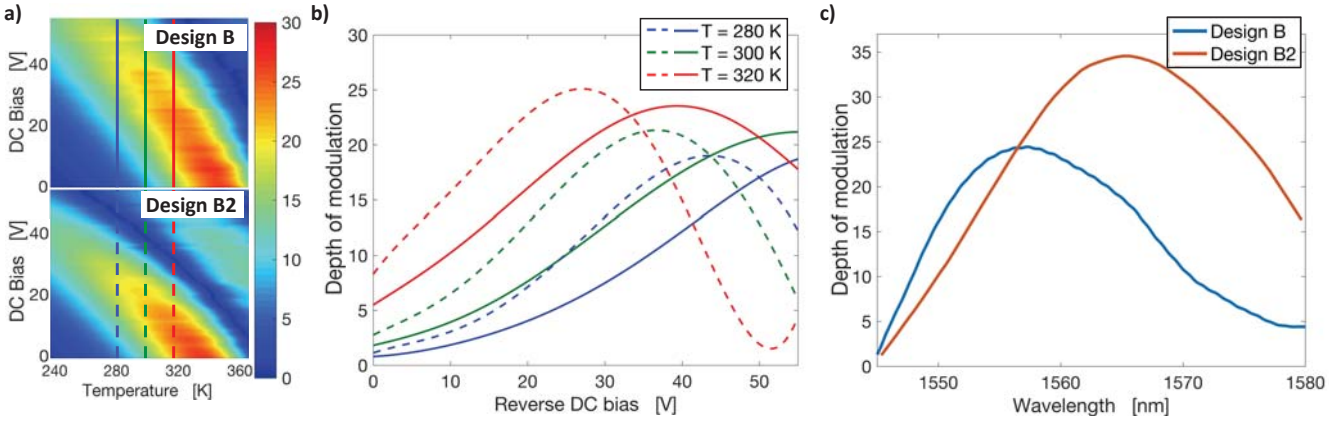

Figure 6 a) Simulated DoM of Design B and B2 as a function of the operating temperature and of the reverse DC bias; b) DoM as a function of reverse DC bias at fixed temperatures of 280 K, 300 K and 320 K, corresponding to the cross sections of a) along the solid and dashed lines, respectively. c) DoM of the fabricated devices of Design B and B2 as a function of wavelength, measured for a 5 V swing from 0 V reverse DC bias.

Therefore, the tradeoff between these two effects yields an optimal device thickness to minimize the depth resolution: this optimal thickness is different for each design. Furthermore, beyond a certain minimum thickness the high field prevents the existence of bound wavefunctions, with a detrimental effect on the DoM. Although, as can be noted from Figure 4a, the minimum depth resolution for *Design B* is slightly better than for *Design B2*, this minimum in fact occurs at an extremely low thickness, which cannot be realized in practice, because of limitations on power consumption and breakdown field. Furthermore, the optimal thickness for *Design B2* corresponds to a power consumption of nearly half of the optimal thickness for *Design B*. This is reflected in Figure 4b, where the inverse of the cost function, Δ, which includes the power consumption, is maximized for a thickness of ~ 5 μm.

One of the key improvements introduced by the optimized designs consists in the capability of achieving a similar modulation performance, at a much lower driving voltage: this is a key factor for the time-of-flight camera application, not only in terms of mere power consumption of the system, but also in terms of heating of the modulator substrate, since in a time-of-flight camera system architecture as that reported in a, cooling of the modulator substrate cannot easily be guaranteed without a detrimental effect on the compactness and overall power consumption of the system. Therefore, since the power consumption is proportional to the square of the voltage swing, as shown in Figure 4c, operation at a lower voltage swing is crucial to reduce the power consumption. This is also shown in Figure 4d, where the inverse of the cost function, Δ, is again maximized for a thickness of ~ 5 μm for all designs.

Moreover, the depth resolution is inversely proportional to the modulation frequency, hence a strategy for improving the system performance is to push the system to work at high frequencies. This however imposes some constraints on the driving circuit, and specifically on the maximum amplitude of the applied AC voltage. It is therefore very rewarding in terms of system performance to seek new QW designs that achieve comparable depth resolution with a smaller applied voltage swing. Figure 4b shows the depth resolution of *Design A2, B* and *B2* as a function of the voltage swing: it is evident that both *Design A2* and *B2* uniformly show a similar depth resolution to that of *Design B* even when operating at a lower voltage swing. Since the modulation frequency is inversely proportional to the depth resolution, this means that the optimized devices could potentially reach sub-cm resolutions at 600 MHz.

B. Experimental results

Several modulator designs like the two discussed above were optimized using the implemented optimization algorithm; considerations on the growth technique and material system, as well as on the robustness of the design, lead to the choice of design B2 to be grown and fabricated for the application in a ToF 3D camera system, as shown in Figure 5.

Figure 6 shows the Depth of Modulation of the optimized *Design B2* and of *Design B* as a function of the temperature, reverse DC bias and wavelength. The reported experimental measurements are in good agreement with what is predicted by the model, confirming that *Design B2* reaches a higher DoM than *Design B*, even for lower applied voltage swing.

The voltage at which the peaks of the DoM occur shifts with a change in temperature: this feature of the SQW design allows a tunability between operating temperature and reverse bias, which is an important advantage of this design over the CQW design. Since the optimization was carried taking into account the performance within the temperature range of interest, Design B2 shows an improved performance with respect to of *Design B* over such range of temperatures. As a result, the DoM peaks are both higher and occur at lower voltages, hence allowing a better adjustment to the operating temperature by tuning the applied bias.

IV. CONCLUSION

In this work we implemented a technique for the systematic optimization of surface-normal electro-absorptive modulators based on the combination of supervised machine learning and analytical modeling. The robustness of the optimization is evaluated using variance-based sensitivity analysis. The capabilities of the developed optimization algorithm were demonstrated for the case of application in a time-of-flight 3D camera system: two novel modulator designs were optimized, showing a significant improvement in the performance of the system, potentially allowing to reach sub-cm depth resolution at 600 MHz. A novel comprehensive figure of merit was proposed, useful for comparing the performance of modulators for application in time-of-flight camera systems and other power-sensitive communication technologies. The proposed technique is highly versatile, and we propose to apply it in future to new material systems and different applications of surface-normal electro-absorptive modulators.

ACKNOWLEDGMENT

We acknowledge the computational resources and staff contributions provided by the Quest high performance computing facility at Northwestern University, which is jointly supported by the Office of the Provost, the Office for Research, and Northwestern University Information Technology.

REFERENCES

[1] G. C. Gilbreath, W. S. Rabinovich, T. J. Meehan, M. J. Vilcheck, M. Stell, R. Mahon, P. G. Goetz, E. Oh, J. A. Vasquez, K. C. R. L. Lucke and S. Mozersky, "Progress in development of multiple-quantum-well retro-modulators for free-space data links," *Optical Engineering*, vol. 42, pp. 1611-1617, 2003.

[2] R. Lange and P. Seitz, "Solid-state time-of-flight range camera," *IEEE Journal of Quantum Electronics*, vol. 37, no. 3, 2001.

[3] G. Ritt and B. Eberle, "Sensor protection against laser dazzling," in *Proceedings of SPIE Vol. 7834*, 2010.

[4] S. Svensson, S. Björkert, H. Kariis and C. Lopes, "Countering laser pointer threats to road safety," in *Proceedings of SPIE Vol. 6402*, 2006.

[5] T. H. Stievater, W. S. Rabinovich, P. G. Goetz, R. Mahon and S. C. Binari, "A surface-normal coupled-quantum-well modulator at 1.55 μm," *IEEE Photonics Technology Letters*, vol. 16, no. 9, 2004.

[6] N. C. Helman, J. E. Roth, D. P. Bour, H. Altug and D. A. B. Miller, "Misalignment-tolerant surface-normal low-voltage modulator for optical interconnects," *IEEE Journal of Selected Topics in Quantum Electronics*, vol. 11, no. 2, 2005.

[7] H. Liu, C. C. Lin and J. S. Harris, "High-speed, dual-function vertical cavity multiple quantum well modulators and photodetectors for optical interconnects," *Optical Engineering*, vol. 40, no. 7, 2001.

[8] H. Mohseni, W. K. Chan, H. An, A. Ulmer and D. Capewell, "Tunable surface-normal modulators operating near 1550 nm with a high-extinction ratio at high temperatures," *IEEE Photonics Technology Letters*, vol. 18, no. 1, 2006.

[9] Y. H. Kuo, Y. K. Lee, Y. Ge, S. Ren, J. E. Roth, T. I. Kaminis and D. A. B. Miller, "Quantum-confined Stark effect in Ge/SiGe quantum wells on Si for optical modulators," *IEEE Journal of Selected Topics in Quantum Electronics*, vol. 12, no. 6, 2006.

[10] H. Mohseni, H. An, Z. A. Shellenbarger, M. H. Kwakernaak and J. H. Abeles, "Enhanced electro-optic effect in GaInAsP-InP three-step quantum wells," *Applied Physics Letters*, vol. 84, no. 11, 2004.

[11] J. Frigerio, V. Vakarin, P. Chaisakul, M. Ferretto, D. Chrastina, X. Le Roux, L. Vivien, G. Isella and D. Marris-Morini, "Giant electro-optic effect in Ge/SiGe coupled quantum wells," *Scientific Reports*, vol. 5, no. 15398, 2015.

[12] H. Mohseni, H. An, Z. A. Sheelenbarger, M. H. Kwakernaak and J. H. Abeles, "Hihgly linear and efficient phase modulators based on GaInAsP-InP three-step quantum wells," *Applied Physics Letters*, vol. 86, no. 031103, 2005.

[13] H. Mohseni, W. K. Chan, H. An, A. Ulmer and D. Capewell, "High-performance optical modulators based on stepped quantum wells," in *Proceedings of SPIE Vol. 6127*, 2006.

[14] D. Zibar, H. Wymeersch and I. Lyubomirsky, "Machine learning under the spotlight," *Nature Photonics*, vol. 11, pp. 745-751, 2017.

[15] I. Hassaninia, R. Bostanabad, W. Chen and H. Mohseni, "Characterization of the optical properties of turbid media by supervised learning of scattering patterns," *Scientific Reports*, vol. 7, no. 15259, 2017.

[16] K. Hujsak, B. D. Myers, E. Roth, Y. Li and V. P. Dravid, "Suppressing electron exposure artifacts: an electron scanning paradigm with bayesian machine learning," *Microscopy and Microanalysis*, vol. 22, pp. 778-788, 2016.

[17] K. Sasikumar, B. Narayanan, M. Cherukara, A. Kinaci, F. G. Sen, S. K. Gray, M. K. Y. Chan and S. K. R. S. Sankaranarayanan, "Evolutionary optimization of a charge transfer ionic potential model for Ta/Ta-oxide heterointerfaces," *Chemisty of Materials*, vol. 29, pp. 3603-3614, 2017.

[18] S. Wheaton, A. Bonakdar, I. Hassaninia, C. L. Tan, V. Fathipour and H. Mohseni, "Open architecture time of flight 3D SWIR camera operating at 150 MHz modulation frequency," *Optics Express*, vol. 25, no. 16, 2017.

[19] I. Hassani Nia, V. Fathipour and H. Mohseni, "Observation of suppressed Auger mechanism in type-I quantum well structures with delocalized electron-

hole wavefunctions," *AIP Advances*, vol. 5, no. 087138-1, 2015.

[20] I. Hassani Nia and H. Mohseni, "A proposal for Coulomb assisted laser cooling of piezoelectric semiconductors," *Applied Physics Letters*, vol. 105, no. 042102, 2014.

[21] I. M. Sobol, "Global sensitivity indices for nonlinear mathematical models and their Monte Carlo estimates," *Mathematics and Computers in Simulation*, vol. 55, pp. 271-280, 2001.

[22] A. Saltelli, P. Annoni, I. Azzini, F. Campolongo, M. Ratto and S. Tarantola, "Variance based sensitivity analysis of model output. Design and estimator for the total sensitivity index," *Computer Physics Communications*, vol. 181, pp. 259-270, 2009.

[23] S. Zlobec, "Characterizing optimality in mathematical programming models," *Acta Applicandae Mathematica*, vol. 12, no. 2, pp. 113-180, 1988.

[24] L. Pavesi, M. Henini and D. Johnston, "Influence of the As overpressure during the molecular beam epitaxy growth of Si-doped (211)A and (311)A GaAs," *Applied Physics Letters*, vol. 66, no. 21, 1995.

[25] T. Y. Lee, Y. J. Lee, D. K. Min, S. H. Lee, W. H. Kim, J. K. Jun, I. Ovsiannikov, Y. G. Jin, Y. Park and E. R. Fossum, "A time-of-flight 3-D image sensor with concentric-photogates demodulation pixels," *IEEE Transactions on Electron Devices*, vol. 61, no. 3, 2014.

Simone Bianconi received his B.S. (2013) and M.S. (2015) degrees in Energy and Nuclear Engineering from University of Bologna, Italy, where he was awarded the Collegio Superiore fellowship. He is currently pursuing a Ph.D. degree in Electrical Engineering, Solid-state and Photonics at Northwestern University. He has been a research assistant with Bio-inspired Sensors and Optoelectronics Lab (BISOL), at Northwestern University since 2016. His research interest includes short-wave infrared single photon detectors and imagers, optical modulators and novel materials for opto-electronics.

Skyler Wheaton received his B.S. in physics from the University of Washington in 2013 and his M.S. in physics from University of Victoria in 2015. He has been a research assistant with Bio-inspired Sensors and Optoelectronics Lab (BISOL), at Northwestern University since 2015. He is interested in novel detectors, optical modulators, optical interrogation, and computational imaging.

[26] Q. Wang, S. Junique, S. Almqvist, D. Agren, B. Noharet and J. Y. Andersson, "1550 nm surface normal electroabsorption modulators for free space optical communications," in *Proceedings of SPIE Vol. 5986*, 2005.

[27] B. E. Clare, K. A. Mudge and K. J. Grant, "Design of a coupled quantum well modulator with enhanced modulation efficiency," in *IQEC/CLEO Pacific Rim*, 2011.

[28] S. Ristic and N. A. F. Jaeger, "Robust coupled-quantum-well structure for use in electrorefraction modulators," *IEEE Electron Device Letters*, vol. 28, no. 1, 2007.

[29] T. H. Stievater, D. Park, M. W. Pruessner, W. S. Rabinovich, S. Kanakaraju and C. J. K. Richardson, "A microelectromechanically tunable asymmetric Fabry-Perot quantum well modulator at 1.55 μm," *Optics Express*, vol. 16, no. 21, 2008.

[30] R. M. Audet, E. H. Edwards, K. C. Balram, S. A. Claussen, R. K. Schaevitz, E. Tasyurek, Y. Rong, E. I. Fei, T. I. Kamins, J. S. Harris and D. A. B. Miller, "Surface-normal Ge/SiGe asymmetric Fabry-Perot optical modulators fabricated on silicon substrates," *Journal of Lightwave Technology*, vol. 31, no. 24, 2013.

Min-Su Park received the B.S. degree from Hongik University and M.S. and Ph.D. degree from Gwangju Institute of Science & Technology (GIST), Republic of Korea, in 2005, 2006, and 2012, respectively. He is currently working as a postdoctoral research fellow in Bio-inspired Sensors and Optoelectronics Lab (BISOL) at Northwestern University. His research interests include optoelectronics and their applications, and also Si-photonics.

Iman Hassani Nia received the B.Sc. and M.Sc. degrees from Shiraz University and his Ph.D. from Northwestern University, Evanston, IL, USA. He is currently a postdoctoral fellow at the Northwestern University. His research interests include optical systems, opto-electronic devices, optical refrigeration, and plasmonic applications. He is an honorary member of American electrochemical society and a Walter Murphy fellow.

This article has been accepted for publication in a future issue of this journal, but has not been fully edited. Content may change prior to final publication. Citation information: DOI 10.1109/JSTQE.2018.2854566, IEEE Journal of Selected Topics in Quantum Electronics

Hooman Mohseni received the Ph.D. degree in electrical engineering from Northwestern University, Evanston, IL, USA, in 2001. He then joined Sarnoff Corporation, where he was a Member of Technical Staff leading several government, domestic, and international commercial projects. He joined Northwestern University as a faculty member in 2004. He is the Director of Bio-Inspired Sensors and Opto-electronics Lab, and Northwestern's Solid-state and Photonics Initiative. He received the Young Faculty Award from Defense Advanced Project Agency in 2007. He was selected by NSF as a US delegates in U.S.-Korea Nanomanufacturing Exchange program in 2007, and US-Japan Young Scientist Exchange Program on Nanotechnology in 2006. He received National Science Foundation's CAREER Award in 2006. He has served as the Advisory Board, the Program Chair, and the Co-chair in several major conferences including IEEE Photonics, SPIE Optics and Photonics, and SPIE Security and Defense. He has published more than 120 peer-reviewed articles in major scientific journals including Nature, Nano Letters, Small, and ACS Nano. He holds 14 issued U.S. and International patents on novel optoelectronic devices and nanoprocessing. He has presented more than 51 invited and keynote talks at different commercial, government, and educational institutes. He is a Fellow of SPIE and a Fellow of Optical Society of America.